Journal of Alloys and Compounds 647 (2015) 364–369

Contents lists available at ScienceDirect

Journal of Alloys and Compounds

journal homepage: http://www.elsevier.com/locate/jalcom

Electronic band structures of binary skutterudites

Banaras Khan [a, b], H.A. Rahnamaye Aliabad [c], Saifullah [a, b], S. Jalali-Asadabadi [d], Imad Khan [a, b], Iftikhar Ahmad [a, b, *]

[a] Center for Computational Materials Science, University of Malakand, Chakdara, Pakistan
[b] Department of Physics, University of Malakand, Chakdara, Pakistan
[c] Department of Physics, Hakim Sabzevari University, Sabzevar, Iran
[d] Department of Physics, Faculty of Science, University of Isfahan (UI), 81744 Isfahan, Iran

ARTICLE INFO

Article history:
Received 11 March 2015
Received in revised form
30 May 2015
Accepted 1 June 2015
Available online 10 June 2015

Keywords:
Binary skutterudites
Thermoelectric materials
Electronic properties
Theoretical condensed matter physics

ABSTRACT

The electronic properties of complex binary skutterudites, MX_3 (M = Co, Rh, Ir; X = P, As, Sb) are explored, using various density functional theory (DFT) based theoretical approaches including Green's Function (GW) as well as regular and non-regular Tran Blaha modified Becke Jhonson (TB-mBJ) methods. The wide range of calculated bandgap values for each compound of this skutterudites family confirm that they are theoretically as challenging as their experimental studies. The computationally expensive GW method, which is generally assume to be efficient in the reproduction of the experimental bandgaps, is also not very successful in the calculation of bandgaps. In this article, the issue of the theoretical bandgaps of these compounds is resolved by reproducing the accurate experimental bandgaps, using the recently developed non-regular TB-mBJ approach, based on DFT. The effectiveness of this technique is due to the fact that a large volume of the binary skutterudite crystal is empty and hence quite large proportion of electrons lie outside of the atomic spheres, where unlike LDA and GGA which are poor in the treatment of these electrons, this technique properly treats these electrons and hence reproduces the clear electronic picture of these compounds.

1. Introduction

The skutterudites family has gained enormous attention as perfect materials in the renewable energy thermoelectric devices. The binary skutterudites display remarkable transport properties, including high degree of carrier's mobility [1]. The unusual transport properties of these compounds are a consequence of the high degree of covalent bonding because of the small electronegativity difference in their constituent elements and narrow bandgaps [1,2]. However, this strong bonding and simple order lead to high lattice thermal conductivity and thus, the issue with them is the reduction of lattice thermal conductivity, which can be resolved by the unique cage like open structure of skutterudites, where the open voids are filled with the rare-earth elements acting as phonon rattlers [1]. The bulk skutterudites with these unique physical properties are considered as ideal materials for thermoelectric applications [3]; although, higher Figure of Merit (ZT) values have been observed in superlattices as compared to bulk materials but superlattices are not useful in large-scale power production due to their high cost and heat transfer; therefore bulk skutterudites with improved ZT values are considered as ideal materials in high-temperature thermoelectric applications [3–7]. These skutterudites are represented by MX_3 (M = Co, Rh, Ir; X = P, As, Sb) having body centered cubic structure with space group $Im\bar{3}$ [8] and crystallize in a cage-like crystal structure, where each transition metal atom is octahedrally coordinated to six pnictide atoms [9,10].

The skutterudite structure is similar to the structure of ReO_3, where perovskite (ABO_3) structure can be attained by introducing void on A site and also the octahedra of the ideal perovskite structure is somewhat tilted [11]. Binary skutterudites are extensively studied materials because of their potential technological applications and diverse physical properties but are challenging for experimentalists as well as theoreticians, due to their narrow bandgaps, complex crystal structure, large unit cell, low symmetry points and strong covalent bonding [12–14]. The complexity of the electronic structure of these compounds can be seen from the bandgap values of the $CoSb_3$. For this compound, the experimentally measured bandgap value varies over a wide range (0.03, 0.04, 0.05, 0.55 and 0.63 eV)

* Corresponding author. Center for Computational Materials Science, University of Malakand, Chakdara, Pakistan.
E-mail address: ahma5532@gmail.com (I. Ahmad).

http://dx.doi.org/10.1016/j.jallcom.2015.06.018
0925-8388/

[15–19]. These differences are due to the difference in the synthesis methods and bandgap measurement techniques. It is obvious that these values are not consistent with each other and similarly the theoretically reported value of the bandgap for this compound using GGA is 0.118 [20], 0.129 [21], 0.036 [22], 0.17 [23] and 0 eV [17], while with LDA is 0 [24] and 0.22 [25] eV. Recently, Hammerschmidt et al. [21] revisited the electronic structure of $CoSb_3$ with different theoretical approaches and obtained bandgaps of 4.17, 0.221, 0.129, 0.089, 0.572 and 0.756 eV by using HF (Hartree Fock), LDA, Perdew-Burke-Enzerhof (PBE), Perdew-Wang 1991 (PW91), Becke-3 Parameter Lee-Yang-Parr (B3LYP) and Becke 3-Pararmetr Perdew-Wang (B3PW) schemes, respectively. Literature reveals similar controversies in the electronic band structures of the other binary skutterudites too. Hence, a comprehensive work on these compounds with great care and reliable theoretical basis is needed to resolve the issue of the theoretical bandgaps of these compounds. In this article, the bandgap structures of these skutterudites compounds are revisited and then various theoretical methods are evaluated to check the best possible theoretical solution for the electronic properties these compounds.

2. Computational details

In the present work we solve the problem with two different approaches. In the first approach self-consistent density functional theory (DFT) calculations are performed using the full potential linearized augmented plane waves plus local orbital (FP-LAPW + lo) method [26] as implemented in the WIEN2k code [27]. For the estimation of the exchange-correlation potential, we use Perdew-Burke-Ernzerhof generalized gradient approximation (PBEsol GGA) [28], regular TB-mBJ [29] and non-regular TB-mBJ [30]. Monkhorst-Pack grid [31] for integrations over the First Brillouin Zone (1BZ) of the unit cell, muffin-tin radii of the elements in compounds and other computational parameters are provided in Table 1. The full relaxations are performed with the criterion of 1 mRy/Bohr on the exerted forces.

For performing the non-regular TB-mBJ calculations, first we determine the correction factor c self-consistently within the regular TB-mBJ calculations. The self-consistently converged values c factor for skutterudites within the regular TB-mBJ calculations are taken small in the first attempt, due to the large electron charge density of these compounds in the interstitial region. To reproduce logical results, we gradually increase the c factor internally for each compound and did not allow its variation during a self-consistent calculation. In this manner the c value is optimized (c_{opt}) for each material and, the calculations performed with the optimized c value are known as non-regular TB-mBJ calculations.

The second approach to solve the problem is GW method, where the GW calculations are performed with the ABINIT code, where this code is based on pseudopotential method and density functional theory is employed to carry out these calculations in a self-consistent manner. In this method, Green's Function approximation (GWA) is used to compute the exchange–correlation energy [32]. In the present calculations, we use FHI (Fritz-Haber-Institute) and Optimized Pseudopotential Interface/Unification Module (OPIUM) generated (Perdew-Burke-Ernzerhof GGA) pseudopotentials [33]. To optimize the structures under study, Hellmann–Feynman forces as small as 10^{-2} eV/Å on each atom are selected. Hedin evaluated the self-energy in GW approximation (GWA) and Hybertsen and Louie applied it by incorporating a Green's function approach [34,35]. The quasiparticle energy E_{nk}^{qp} as a GGA energy eigenvalue plus a many body correction is calculated using the following equation:

$$E_{nk}^{qp} = \varepsilon_{nk}^{GGA} + \left\langle n\vec{k}\left| \sum\left(E_{nk}^{qp}\right) - V_{xc}^{GGA}\right| n\vec{k}\right\rangle \quad (1)$$

where ε_{nk}^{GGA} is the nth energy level at wave number k, V_{xc}^{GGA} is the exchange–correlation potential in GGA and $\sum(E_{nk}^{qp})$ is the self-energy for the quasiparticle energy E_{nk}^{qp} [36].

3. Results and discussions

One of the most fundamental parameter which describes many physical properties of a compound is the bandgap. Bandgap of a material provides a detailed account of the optical, electronic, opto-electronic and thermoelectric properties of that material. Therefore, the knowledge of the electronic structure of a material is necessary for its possible technological applications in various devices. In optoelectronics we are mostly concerned with direct bandgap materials, where the gap value in the range of infrared (IR) to ultraviolet (UV) depends strictly upon the nature of application. Though, there are more stringent requirements for efficient thermoelectric materials but unlike optically active materials, they require narrow bandgap compounds irrespective of their nature, direct or indirect.

The measurement of the optical properties of a material directly investigates its electronic structure and hence provides valuable information about the band structure of that compound [37]. Thus these measurements estimate the energy difference between the valence and conduction bands, i.e. bandgap (E_g), which is used to determine the electronic and thermoelectric properties materials [38]. Different experimental methods are used to measure bandgaps of semiconductors but the best values are generally obtained by optical absorption [39]. In Table 2, we have presented the experimental bandgaps of the binary skutterudites obtained by different experimental techniques. For reliability as well as rational and logical discussion on the electronic structure of the binary skutterudites, we will follow the results obtained by the optical absorption techniques, i.e., 0.45 [40], 0.43 [19], 0.69 [19], 0.63 [19], 1.4 [41], 0.8 [19] and 0.8

Table 1
Computational parameters.

Compound	k-points meshes	$R_{MT}K_{MAX}$	Separation energy (Ry)	G_{MAX} ($Ry^{1/2}$)	Muffin-tin radii (a.u.)	
					M	X
MX_3						
CoP_3	23 × 23 × 23	5.5	−6.0	12	2.33	1.81
$CoAs_3$	23 × 23 × 23	5.5	−6.0	12	2.00	2.11
$CoSb_3$	23 × 23 × 23	5.5	−6.0	12	2.30	2.35
IrP_3	23 × 23 × 23	5.5	−6.0	12	2.41	1.78
$IrAs_3$	23 × 23 × 23	5.5	−6.0	12	2.32	2.21
$IrSb_3$	23 × 23 × 23	5.5	−6.0	12	2.39	2.27
RhP_3	23 × 23 × 23	5.5	−6.0	12	2.47	1.92
$RhAs_3$	23 × 23 × 23	5.5	−6.0	12	2.32	2.21
$RhSb_3$	23 × 23 × 23	5.5	−6.0	12	2.33	2.33

Table 2
Comparison of calculated bandgaps (in eV) using GW, LDA and GGA with the experimental results for binary skutterudites.

Compound	Experimental	LDA	GGA	GW
CoP_3	0.45[a], 0.43[b]	metal[n,l,f,g]		0.592
$CoAs_3$	0.69[b]	0[h,l]	0.337[e], 0[h]	0.045
$CoSb_3$	0.55[c], 0.63[b],0.05[t], 0.031[o], 0.04[r]	0[h], 0.22[i], 0.221[k],0.003[l]	0.118[i], 0.129[k], 0.036[p], 0.17[j],0[t]	0.335
IrP_3	sc[b]	0.136[l]		0.119
$IrSb_3$	1.4[d], 1.18[s]	0[h], 0.075[l]	0[i,t]	0.086
$IrAs_3$	sc[b]	0.156[l]		0.635
RhP_3	metal[b,q]	metal[l]		0.123
$RhAs_3$	0.8[b]	0[l]		0.214
$RhSb_3$	0.8[c]	metal[l], 0[m]	0[i]	0.165

sc semiconductor.
[a] Ref. [40].
[b] Ref. [19].
[c] Ref. [18].
[d] Ref. [41].
[e] Ref. [24].
[f] Ref. [47].
[g] Ref. [48].
[h] Ref. [23].
[i] Ref. [20].
[j] Ref. [25].
[k] Ref. [21].
[l] Ref. [49].
[m] Ref. [10].
[n] Ref. [50].
[o] Ref. [15].
[p] Ref. [22].
[q] Ref. [51].
[r] Ref. [16].
[s] Ref. [52].
[t] Ref. [17].

[18] eV values for CoP_3, $CoAs_3$, $CoSb_3$, $IrSb_3$, $RhAs_3$ and $RhSb_3$, respectively and hence will compare other theoretical results.

Table 2 clearly indicates that the bandgaps obtained by the theoretical approaches of local density approximation (LDA) and generalized gradient approximation (GGA) are severely underestimated. Therefore LDA and GGA methods are not successful in reproducing the correct bandgaps of the binary skutterudite compounds. This is due to the fact that the bonding nature of these binary skutterudites is covalent and due to this covalent nature charge leakage occurs from their muffin-tin (MT) radii to the interstitial regions. Therefore the correct electronic structure calculations of these compounds is not possible for the theoretical techniques LDA and GGA, where these techniques are suitable for situations if charge leakage from MT sphere is less and maximum of the charge is localized inside the MT spheres.

The poor bandgaps by the LDA and GGA are not unexpected, as these approaches are not useful for the open-shell 3d, 4d, 5d, 4f, or 5f orbitals. In other words the main reasons for the ineffectiveness, of these DFT based methods to these compounds, are their large unit cells, hollow spaces in the unit cells, narrow bandgaps, complex crystal structures, strongly correlated natures due to the transition metals d states, low symmetry points and strong covalent bonding. Therefore, because of these complexities the theoretical handling of these materials is as complicated as their experimental treatment and therefore, one needs to think beyond the LDA and GGA methods. Hence, these compounds need extensive care and experience of the pros and cons of the different theoretical methods in order to reproduce the experimental bandgaps of these skutterudites.

Keeping all these complexities of these compounds in mind we approached to address the issue of the theoretical bandgaps of these compounds, with the computationally expensive but reliable theoretical tool, GW method. Our calculated bandgaps with the GW method are presented in Table 2. Fig. 1 also shows a comparison of the calculated bandgaps with the experimental results. Experimental bandgaps are taken along abscissa while theoretical bandgaps are taken along ordinate. Along the ordinate the theoretical values of bandgaps are taken for the approaches LDA, GGA, GW, TB-mBJ and non-regular TB-mBJ. It is clear from the table as well as Fig. 1, that the calculated bandgap for CoP_3 with GW 0.592 eV is consistent with the experimentally reported result of 0.45 eV [40] and 0.43 eV [19]. However, the values obtained by the GW for the other skutterudites 0.045, 0.335, 0.086, 0.123, 0.214 and 0.165 eV are not much impressive and results are far away from the experimental values 0.69 eV [19], 0.63 eV [19], 1.4 eV [41], 0 eV [19], 0.8 eV [19], 0.8 eV [18] for $CoAs_3$, $CoSb_3$, $IrSb_3$, RhP_3, $RhAs_3$ and $RhSb_3$ respectively, which reveals that even this computationally expensive and reliable GW technique is also not a good choice for the prediction of the bandgaps of these binary skutterudites.

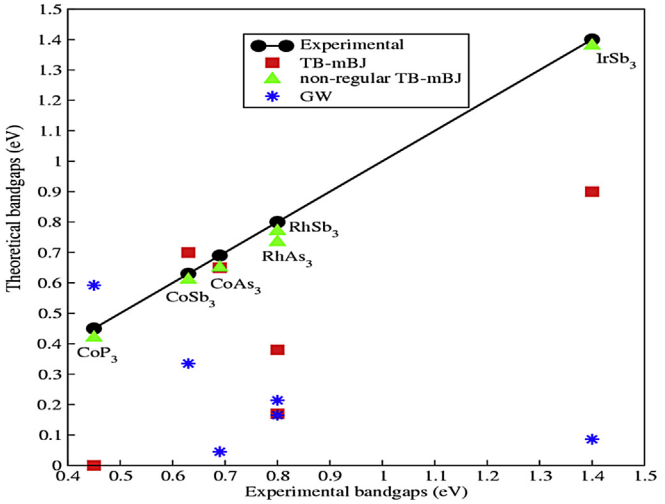

Fig. 1. Comparison of calculated bandgaps (ordinate) by GW, TB-mBJ and non-regular TB-mBJ with the experimental bandgaps (abscissa) for binary skutterudites.

Table 3
Comparison of the calculated bandgaps (eV) using TB-mBJ and non-regular TB-mBJ methods with the experimentally measured bandgaps by optical techniques.

Compound	Optical bandgap	TB-mBJ	Non-regular TB-mBJ	C_{opt} factor	Bandgap nature
CoP_3	0.45[a], 0.43[b]	0.00	0.42	1.5007	Indirect
$CoAs_3$	0.69[b]	0.65	0.65	1.2122	Indirect
$CoSb_3$	0.63[b]	0.58	0.61	1.5099	Indirect
IrP_3	sc[b]	0.61	0.61	1.1948	Indirect
$IrSb_3$	sc[b]	0.87	0.87	1.4711	Indirect
$IrAs_3$	1.40[c]	0.90	1.38	1.5495	Indirect
RhP_3	metal[b]	metal	metal	1.1777	Metal
$RhAs_3$	0.80[b]	0.38	0.77	1.6203	Indirect
$RhSb_3$	0.80[d]	0.17	0.73	1.7451	Indirect

sc semiconductor.
[a] Ref. [40].
[b] Ref. [19].
[c] Ref. [18].
[d] Ref. [41].

The binary skutterudites have large unit cells and large amount of free space is available in their crystals because of the missing positions in the perovskite like structure. The other available theoretical methods like LDA and GGA are not efficient in the treatment of the electrons reside in the voids in these compounds, whereas these electrons can be properly treated by the TB-mBJ method. Therefore, we approached to the problem with the recently developed Tran and Blaha modified Becke and Johnson (BJ) exchange potential (TB-mBJ). The inherent limitations of the density functional theory are reduced by Tran and Blaha via the modification of the Becke and Johnson (BJ) exchange potential [42]. This theoretical method (TB-mBJ) is very efficient for the bandgaps and the effectiveness of this approach can be found in a wide range of compounds [43–46].

The calculated bandgaps by the regular TB-mBJ are presented in Table 3. It is clear from Tables 2 and 3 as well as Fig. 2 that the bandgaps calculated by the regular TB-mBJ for the binary skutterudite compounds MX_3 (M = Co, Rh, Ir; X = P, As, Sb) are better than that of the LDA and GGA approaches but are inferior than the pseudopotential GW method. The results obtained by the regular TB-mBJ also show serious under estimation when compared to the experimental results.

Recently the TB-mBJ approach is further improved by the re-parameterization of the correction c-factor [30]. The TB-mBJ exchange potential is:

$$\upsilon_{x,\sigma}^{TB-mBJ}(\mathbf{r}) = \left(1.023\sqrt{\frac{1}{\Omega}\int_{\Omega}\frac{|\nabla\rho_\sigma(\mathbf{r}')|d\mathbf{r}'}{\rho_\sigma(\acute{r})}} - 0.012\right) \times \left\{\frac{2\sqrt[3]{\pi\rho_\sigma(\mathbf{r})}e^{x_\sigma(\mathbf{r})/3}}{x_\sigma(\mathbf{r})}\left[\left(1+\frac{1}{2}x_\sigma(\mathbf{r})\right)e^{-x_\sigma(\mathbf{r})}-1\right] + \frac{3}{\pi}\sqrt{\frac{5}{12}}\left(\frac{\sum_{i=1}^{N_\sigma}\nabla\Psi_{i,\sigma}^*\cdot\nabla\Psi_{i,\sigma}}{\sum_{i=1}^{N_\sigma}|\Psi_{i,\sigma}|^2}\right)^{1/2}\right\} - \frac{2}{\pi}\sqrt{\frac{5}{12}}\left(\frac{\sum_{i=1}^{N_\sigma}\nabla\Psi_{i,\sigma}^*\cdot\nabla\Psi_{i,\sigma}}{\sum_{i=1}^{N_\sigma}|\Psi_{i,\sigma}|^2}\right)^{1/2} \quad (2)$$

$$\upsilon_{x,\sigma}^{TB-mBJ}(\mathbf{r}) = c\times\left(\upsilon_{x,\sigma}^{BJ}(\mathbf{r}) + \frac{1}{\pi}\sqrt{\frac{10t_\sigma(\mathbf{r})}{3\rho_\sigma(\mathbf{r})}}\right) - \frac{1}{\pi}\sqrt{\frac{10t_\sigma(\mathbf{r})}{3\rho_\sigma(\mathbf{r})}} \quad (3)$$

where Ω is the unit cell volume, and x_σ is related to the topology of the electron charge density, which can be obtained from the electron charge density $\rho_\sigma(\mathbf{r}) = \sum_{i=\sigma}^{N_\sigma}|\Psi_{i,\sigma}|^2$, $\nabla\rho_\sigma$ and $\nabla^2\rho_\sigma$ are the gradient and Laplacian of the electron charge density and $t_\sigma(\mathbf{r}) = \frac{1}{2}\sum_{i=1}^{N_\sigma}\nabla\Psi_{i,\sigma}^*\cdot\nabla\Psi_{i,\sigma}$ is the electron kinetic-energy density. The two parameters, 1.023 *Bohr* and −0.012 (dimensionless), in the first parenthesis of Eq. (2) are optimized by Tran and Blaha in order to reproduce the experimental bandgaps of several compounds including wide bandgap insulators, sp semiconductors, and strongly correlated 3d transition-metal oxides.

The $\upsilon_{x,\sigma}^{TB-mBJ}(\mathbf{r})$ exchange potential is represented versus the $\upsilon_{x,\sigma}^{BJ}(\mathbf{r})$ exchange potential as shown in Eq. (3), where c is the expression given in the first parenthesis of Eq. (2). Therefore, if c = 1, then $\upsilon_{x,\sigma}^{TB-mBJ}(\mathbf{r}) = \upsilon_{x,\sigma}^{BJ}(\mathbf{r})$ is consistent with Ref. 33 and Ref. 35. It clarifies that why one needs to perform regular LDA or GGA calculations to carry out the TB-mBJ calculations. The $\upsilon_{x,\sigma}^{TB-mBJ}(\mathbf{r})$ potential, as can be seen from Eqs. (2) and (3), is introduced directly and not obtained from an exchange energy functional E_x.

Generally, the TB-mBJ method is not very efficient in hollow compounds and more elaborations are needed in the form of non-regular TB-mBJ method to reproduce correct experimental bandgaps for such compounds. It is clear from Eq. (2) that c factor is linearly dependent on the square root of $\frac{|\nabla\rho_\sigma|}{\rho_\sigma}$. The relation shows that the bandgap value increases as c increases. The TB-mBJ method could not reproduce the correct experimental bandgaps for binary skutterudites due to their large electron charge density in the interstitial region caused by the empty space because of the missing sites in the pervoskite like structure. To improve the results of the TB-mBJ method and reproduce the experimental band gaps for these compounds we approach with a non-regular TB-mBJ (nTB-mBJ) scheme, where in this scheme c-parameter is optimized for each compound and its optimum values (c_{opt}) is used in the nTB-mBJ calculations. The optimized values of the c-factor for all the compounds are presented in Table 3.

Fig. 2 shows the calculated band structures of $RhAs_3$, $RhSb_3$ and $IrSb_3$ by using the nTB-mBJ approach. The calculated bandgap values for the binary skutterudite compounds with the non-regular TB-mBJ method are compared with the regular TB-mBJ and GW methods, as well as, the experimentally measured results by optical methods in Fig. 1 and Table 3. It is clear from the figure and table that the calculated bandgap values via non-regular TB-mBJ are consistent to the experimental results. This indicates that the non-regular TB-mBJ is an efficient theoretical tool to deal with such kind

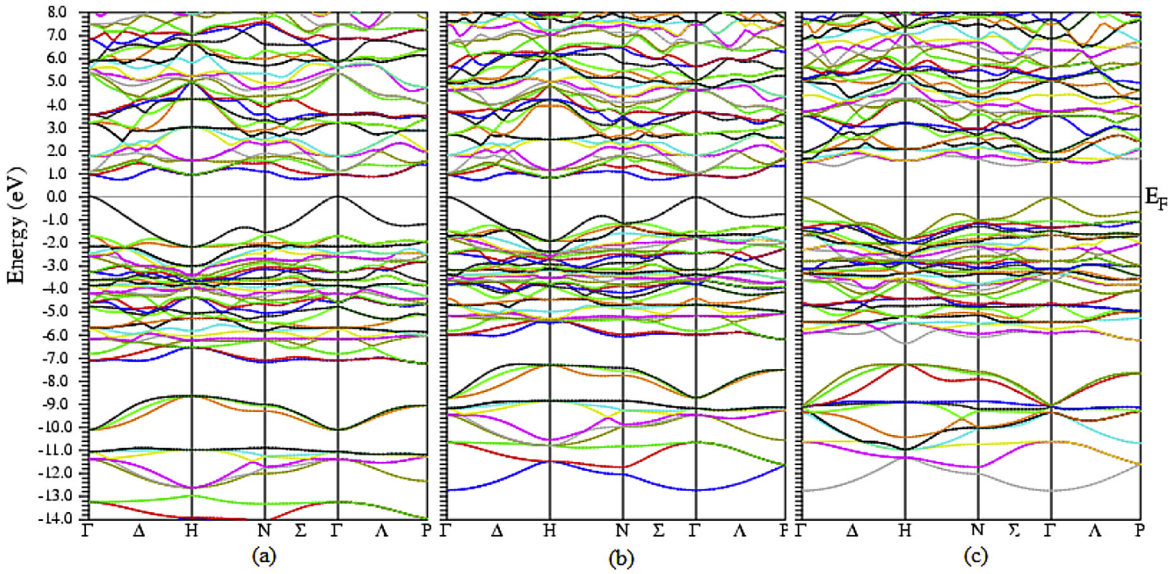

Fig. 2. Calculated band structures of (a) $RhAs_3$ (b) $RhSb_3$ and (c) $IrSb_3$ by using the non-regular TB-BJ approach.

of problems. It is important to be noted that GW calculations are computationally expensive and generally reliable, but for these compounds the non-regular TB-mBJ performance is not only better than LDA, GGA and regular TB-mBJ but also than the GW calculations.

The effectiveness of the TB-mBJ, in the electronic structure calculations for the skutterudites, confirms that the charge leakage in these compounds from the muffin-tin radii to the interstitial site is large and the contribution of the interstitial states is found to be comparable to that of the muffin-tin spheres. As the majority of the electrons in these skutterudites are not limited to muffin-tin spheres therefore they cannot be properly treated with the LDA and GGA within the APW-based methods, which are somewhat effective schemes for the situations where orbitals are more or less localized in atomic spheres. This establishes a fact of the better performance of the non-regular TB-mBJ scheme for the skutterudites family as compared to the other theoretical approaches.

4. Conclusions

In summary, we have performed the electronic structure calculations of the challenging compounds, binary skutterudites MX_3 (M = Co, Rh, Ir; X = P, As, Sb), with various theoretical approaches, i.e., regular TB-mBJ, non-regular TB-mBJ and GW methods. The calculated results are also compared with the available results of the LDA and GGA methods. It is concluded that the electronic band structures are severely underestimated by LDA and GGA form the corresponding experimental results, as these techniques work well for materials in which electrons are limited to atomic spheres, but in these skutterudites quite large proportion of electrons are out of atomic spheres and hence cannot be properly treated by these methods. The GW and TB-mBJ methods though reproduce reasonable bandgaps for these compounds but are still somewhat inconsistent with the experimental results. It is further concluded that the non-regular TB-mBJ reproduces the correct experimental bandgaps for these compounds and hence is a suitable theoretical approach for these skutterudites and related complex structured challenging compounds, which have large amount of voids. The root cause for the effectiveness of this technique is the proper treatment of electrons, both in the muffin tin spheres of atoms and interstitial regions.

References

[1] G.J. Snyder, E.S. Toberer, Nat. Mater. 7 (2008) 105–114.
[2] B.C. Sales, D. Mandrus, R.K. Williams, Science 272 (1996) 1325–1328.
[3] B. Poudel, Q. Hao, Y. Ma, Y. Lan, A. Minnich, B. Yu, X. Yan, D. Wang, A. Muto, D. Vashaee, X. Chen, J. Liu, M.S. Dresselhaus, G. Chen, Z. Ren, Science 320 (2008) 634–638.
[4] R. Venkatasubramanian, E. Siivola, T. Colpitts, B. O'Quinn, Nature 413 (2001) 597–602.
[5] T.C. Harman, P.J. Taylor, M.P. Walsh, B.E. LaForge, Science 297 (2002) 2229–2232.
[6] K.F. Hsu, S. Loo, F. Guo, W. Chen, J.S. Dyck, C. Uher, T. Hogan, E.K. Polychroniadis, M.G. Kanatzidis, Science 303 (2004) 818–821.
[7] J.-P. Fluerial, T. Caillat, A. Borshchevsky, in: Proceedings of the 13th International Conference on Thermoelectrics, Kansas City, MO, 30 August to 1 September 1994 (AIP, New York), 1995, pp. 40–44.
[8] L. Kumari, W. Li, J.Y. Huang, P.P. Provencio, Nanoscale Res. Lett. 5 (2010) 1698–1705.
[9] K. Akai, K. Oshiro, M. Matsuura, in: Proceedings of the 18th International Conference on Thermoelectrics, Baltimore, 1999, p. 444.
[10] M. Fornari, D.J. Singh, Appl. Phys. Lett. 74 (1999) 3666–3668.
[11] D. Jung, M.H. Whangbo, S. Alvarez, Inorg. Chem. 29 (1990) 2252–2255.
[12] G.D. Mahan, H. Ehreinreich, F. Spaepen (Eds.), Solid State Physics, vol. 51, Academic Press, New York, 1998, p. 81.
[13] D.J. Singh, Semicond. Semimet. 70 (2001) 125.
[14] M.S. Schmøkel, L. Bjerg, J. Overgaar, F.K. Larsen, G.K.H. Madsen, K. Sugimoto, M. Takata, B.B. Iversen, Angew. Chem. Int. Ed. 52 (2013) 1503–1506.
[15] E. Arushanov, M. Respaud, H. Rakoto, J.M. Broto, T. Caillat, Phys. Rev. B 61 (2000) 4672–4676.
[16] H. Ishii, K. Okazaki, A. Fujimori, Y. Nagamoto, T. Koyanagi, J.O. Sofo, J. Phys. Soc. Jpn. 71 (2002) 2271–2275.
[17] J. Nagao, M. Ferhat, H. Anno, K. Matsubara, E. Hatta, K. Mukasa, Appl. Phys. Lett. 76 (2000) 3436–3438.
[18] G.S. Nolas, G.A. Slack, T. Caillat, G.P. Meisner, J. Appl. Phys. 79 (1996) 2622–3262.
[19] J.-P. Fleurial, T. Caillat, A. Borshchevsky, in: Proceedings ICT '97. XVI International Conference on Thermoelectrics IEEE, Dresden, Germany, August 26-29, 1997, pp. 1–11.
[20] K. Koga, K. Akai, K. Oshiro, M. Matsuura, Phys. Rev. B 71 (2005) 155119–155128.
[21] L. Hammerschmidt, S. Schlecht, B. Paulus, Phys. Status Solidi A 210 (2013) 131–139.
[22] H.A.R. Aliabad, M. Ghazanfari, I. Ahmad, Comp. Mat. Sci. 65 (2012) 509–519.
[23] D.J. Singh, W.E. Pickett, Phys. Rev. B 50 (1994) 11235–11238.
[24] K. Takegahara, H. Harima, Internal Parameter Dependence of Electronic Band Structure for $CoAs_3$, Proceedings.
[25] J.O. Sofo, G.D. Mahan, Phys. Rev. B 58 (1998) 15620–15623.
[26] E. Sjostedt, L. Nordstrom, D.J. Singh, Solid State Commun. 114 (2000) 15–20.
[27] P. Blaha, K. Schwarz, G.K.H. Madsen, D. Kvasnicka, L. Luitz, WIEN2k User's Guide, Vienna University of Technology, 2011, ISBN 3-9501031-1-2.
[28] J.P. Perdew, A. Ruzsinszky, G.I. Csonka, O.A. Vydrov, G.E. Cuseria, L.A. Constantin, X. Zhou, K. Burke, Phys. Rev. Lett. 100 (2008) 136406–136410.
[29] F. Tran, P. Blaha, Phys. Rev. Lett. 102 (2009) 226401–226405.

[30] D. Koller, F. Tran, P. Blaha, Phys. Rev. B 85 (2012) 155109–155117.
[31] H.J. Monkhurst, J.D. Pack, Phys. Rev. B 13 (1976) 5188–5192.
[32] X. Gonze, J.M. Beuken, R. Caracas, F. Detraux, M. Fuchs, G.M. Rignanese, L. Sindic, M. Verstraete, G. Zerah, F. Jollet, M. Torrent, A. Roy, M. Mikami, P. Ghosez, J.Y. Raty, D.C. Allan, Comput. Mater. Sci. 25 (2002) 478–492.
[33] E.J. Walter, Optium-Pseudopotential Generation Project, http://opium.sourceforge.net/guide.html.
[34] L. Hedin, Phys. Rev. 139 (1965) A796–A823.
[35] M.S. Hybertsen, S.G. Louie, Phys. Rev. B 34 (1986) 5390–5413.
[36] P.S. Yadav, R.K. Yadav, S. Agrawal, B.K. Agrawal, Phys. E 36 (2007) 79–85.
[37] C.E. Ekuma, D.J. Singh, J. Moreno, M. Jarrell, Phys. Rev. B 85 (2012) 085205–085212.
[38] H.J. Goldsmid, Introduction to Thermoelectricity, Springer Series in Material Science, 121, Springer, Berlin, 2010, ISBN 978-3-642-00715-6, p. 42.
[39] C. Kittel, Introduction to Solid State Physics, Eight Edition, 188, 2005, ISBN 0-471-41526-X.
[40] J. Ackermann, A. Wold, J. Phys. Chem. Solids 38 (1977) 1013–1016.
[41] G.A. Slack, V.G. Tsoukala, J. Appl. Phys. 76 (1994) 1665–1671.
[42] A.D. Becke, E.R. Johnson, J. Chem. Phys. 124 (2006) 221101–221105.
[43] D. Koller, F. Tran, P. Blaha, Phys. Rev. B 83 (2011) 195134–195144.
[44] I. Khan, I. Ahmad, H.A.R. Aliabad, M. Maqbool, J. Appl. Phys. 112 (2012) 073104–073111.
[45] I. Khan, I. Ahmad, Int. J. Quantum Chem. 113 (2013) 1285–1292.
[46] I. Khan, I. Ahmad, D. Zhang, H.A.R. Aliabad, S.J. Asadabadi, Phys. Chem. Solids 74 (2013) 181–188.
[47] H. Harima, Prog. Theor. Phys. (2000) 117–118. Supplement No. 138.
[48] M. Llunell, P. Alemany, S. Alvarez, V.P. Zhukov, A. Vernes, Phys. Rev. B 53 (1996) 10605–10609.
[49] K. Takegahara, H. Harima, Phys. B 328 (2003) 74–76.
[50] M. Fornari, D.J. Singh, Phys. Rev. B 59 (1999) 9722–9724.
[51] J.P. Odile, S. Soled, C.A. Castro, A. Wold, Inorg. Chem. 17 (1978) 283–286.
[52] T. Caillat, A. Borshochevsky, J.-P. Fleurial, AIP Conf. Proc. 316 (1994) 31.